

Red Blood Cell Segmentation with Overlapping Cell Separation and Classification on Imbalanced Dataset

Korranat Naruenatthanaset¹, Thanarat H. Chalidabhongse^{1,2}, Duangdao Palasawan³,
Nantheera Anantrasirichai⁴, and Attakorn Palasawan³

Abstract— Automated red blood cell classification on blood smear images helps hematologist to analyze RBC lab results in less time and cost. Overlapping cells can cause incorrect predicted results that have to separate into multiple single RBCs before classifying. To classify multiple classes with deep learning, imbalance problems are common in medical imaging because normal samples are always higher than rare disease samples. This paper presents a new method to segment and classify red blood cells from blood smear images, specifically to tackle cell overlapping and data imbalance problems. Focusing on overlapping cell separation, our segmentation process first estimates ellipses to represent red blood cells. The method detects the concave points and then finds the ellipses using directed ellipse fitting. The accuracy is 0.889 on 20 blood smear images. Classification requires balanced training datasets. However, some RBC types are rare. The imbalance ratio is 34.538 on 12 classes with 20,875 individual red blood cell samples. The use of machine learning for RBC classification with an imbalance dataset is hence more challenging than many other applications. We analyze techniques to deal with this problem. The best accuracy and f1 score are 0.921 and 0.8679 on EfficientNet-b1 with augmentation. Experimental results show that the weight balancing technique with augmentation has the potential to deal with imbalance problems by improving the f1 score on minority classes while data augmentation significantly improves the overall classification performance.

I. INTRODUCTION

Red blood cells (RBCs) are the most abundant cell in blood fluid, which have red blood cells, white blood cells, platelets, and plasmas. The main roles of RBC are to transport oxygen from the lungs to the entire body and carry carbon dioxide from the body to the lungs via blood vessels. In a hospital, RBC morphology analysis is a subprocess in the Complete Blood Count (CBC) process. The analysis plays an essential role in diagnosing many diseases, caused by RBC disorder such as anemia, thalassemia, sickle cell disease, etc. It mainly focuses on shape, size, color, inclusions, and arrangement of RBC [1]. Generally, normal RBC shape is round, biconcave with pale central pallor. It has 6 – 8 μm diameter. A hematologist manually analyzes the blood cells through a microscope from blood smear slides. This manual inspection is a long process and also needs practices and experiences. Since recent computer vision and image processing in the medical imaging area provide efficient tools, it can help

hematologists automatically analyze RBC images from a microscope in less time and cost.

Most of the studies in the RBC image area is to classify RBCs, identify the type of RBCs in the image. Normally, the image, captured from a microscope, contains many cells so it has to segment the cell before the classification process. Recent studies in RBC classification, it mostly uses deep learning techniques which they were shown state-of-the-art (SOTA) results in image classification in recent year. However, there are several challenges to achieve the goal. RBCs in the image may overlap with each other which is hard to find the edge of the cell. In the manual process, hematologist usually avoids selecting the area that has a lot of overlapping cells. But in some situations, especially for automated method, it difficult to avoid because the cells are stick together making wrong predicted results. Automated segmentation must handle the overlapping cells so it can cover the real situation. Blood smear slides may not have the same environment such as lighting, zoom scale, and camera. Since deep learning technique shows the remarkable result in computer vision, Researchers need lots of data to perform good outcome. Nevertheless, the RBC dataset is difficult to collect because some RBC types can find only in the specific disease, which was found in the specific regions. Accordingly, the dataset usually has an imbalance problem. Moreover, to label the data, it needs a specialist to label it into the correct type, even different specialists might give different results, depending on expertise.

This paper presents a new framework for RBC segmentation using ellipse fitting and classification using EfficientNet [2]. The main contributions of the paper are: i) a new method to separate the overlapping cells based on concave points of the border of RBCs; ii) RBC classification with analysis of imbalanced datasets using data augmentation, weight normalization, upsampling, and Focal loss [3] on multi-class classification.

II. RED BLOOD CELL COUNTS AND THE AUTOMATE METHODS

Blood smear image studies in computer vision area usually target on a specific cell: white blood cell, red blood cell, and platelet [4]. automate counting and classification of RBCs can be used in Complete Blood Count (CBC) test or specific disease diagnoses such as malaria, leukemia, and anemia. Counting in each abnormal RBC types show signs of disease and level of critical illness which observed by hematologist. In this section, previous RBC studies were reviewed.

¹Department of Computer Engineering, Chulalongkorn University, Bangkok, Thailand

²Research Group on Applied Computer Engineering Technology for Medicine and Healthcare, Chulalongkorn University, Bangkok, Thailand

³Cell Disorders Research Unit, Department of Clinical Microscopy, Faculty of Allied Health Sciences, Chulalongkorn University, Bangkok, Thailand

⁴Visual Information Laboratory, University of Bristol, Bristol BS8 1UB, UK

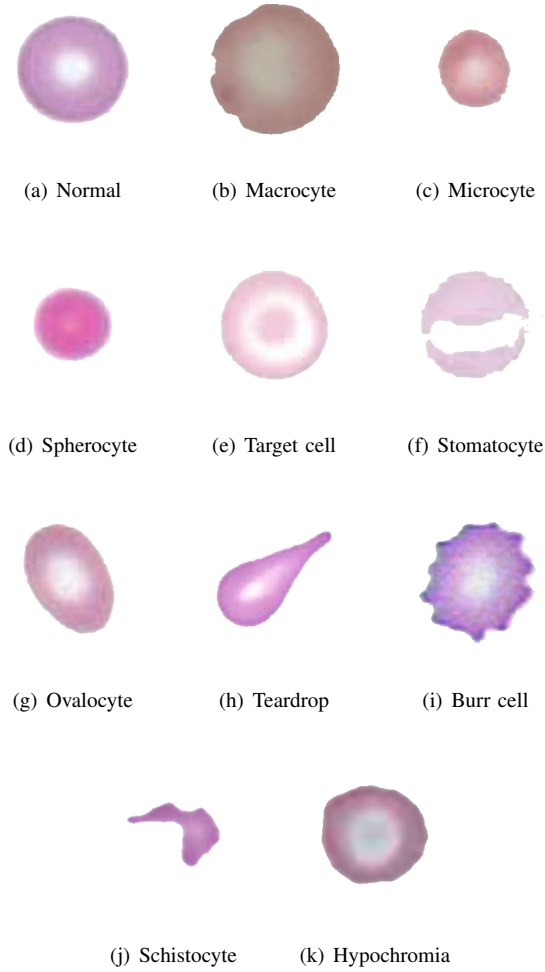


Fig. 1. RBCs types

A. Red Blood Cell types

12 RBC types were focused in this study as shown in figure 1. As observed RBC from blood smear slide in a microscope, normal RBCs are a red circle with a white pale circle in the middle called central pallor which is the most cells found in a healthy body. But for abnormal RBCs, it looks different from the normal in shape, size, color, inclusion, and arrangement [1]. Each type of abnormal RBCs can be found in various types of diseases. (b) and (c) in figure 1 are bigger and smaller than the normal. (d) - (f) and (k) can be distinguished by observing central pallor. (g) - (i) are different in the shape of the cells. (j) is a fragmented RBC. Therefore, inclusion RBC, which is the RBCs with dark dots inside such as malaria parasite, is not focused on this study. However, a single RBC might contain more than one characteristic type: Oval + Macrocyte, Hypochromia + Macrocyte. Although Our classification studies is a multi-class classification, which 1 RBC has only 1 class.

B. Segmentation

Lower RBCs cause unhealthy and many symptoms such as anemia, normally 4.7 - 6.1 million cells per microlitre in men and 4.2 - 5.4 million cells per microlitre in women. RBC counting in each type is a subprocess in Complete Blood Count (CBC). Hematologist approximately total count in each type from multiple blood smear slides. Automate RBC counting firstly occurred only focus on the

number of the RBCs. After that, precise shape extraction study was focused for using in classification step. The automated process usually starts with converting color image to a grayscale of blood smear images. Then, preprocessing is done to improve contrast and reduce noise. Next, segmentation step is applied following by morphology operation to extract RBC contours. The difference method were used in the segmentation step. To identify a number of RBCs, circle Hough transform was used which works good for circular shape similar to RBCs [5], [6]. To extract the precise RBC shape, Otsu thresholding [7], [8], [9], [10], [11], [12], [13], [14] usually was used in many studies due to highly contrast between RBC area and background. For edge detection, Canny edge detection [15], [16] and Sobel edge detection [17] also were used in this task. There are studies using other methods: Dijkstra's shortest path on RBC border [18], ring shape dilation to identify RBCs [19], Watershed [20], [21], Active appearance model on sliding windows [22], K-means [23], and histogram equalization [24]. The most recent studies used fully convolutional neural network (FCN), FCN-Alexnet [25] and deformable U-net [26].

The segmentation can contain overlapping cells. To classify RBC, it mostly needs to separate into single cells to compute features or feed into the deep learning model. Addition step after segmentation was done to separated overlapping cells. Circle Hough transform can used to estimate RBCs in contour [21], [6]. Most studies identify a number of RBCs in contour then segment the area of each cells. Distance transform was used to find peak spot as markers of RBCs then Watershed [14], or random walk method [27] was applied. [11] used an area to determine a number of RBCs in contour, then used K-means on pixel coordinates. [28] also purpose overlapping cell separation using ellipse adjustment with concave point finding.

According to the previous studies, several methods that extract RBC from the background give good results because RBCs usually have high contrast. However, it difficult to find the best algorithm to separate the cells that connect to each other, because the overlapping cells can have complex shapes. The watershed method can perform good results on the overlapping cells that remain space between the center in each cell, while ellipse adjustment needs concave areas between cells. Also, the FCN methods are good to segment the cells due to the quality and number of datasets and labels, but it cannot separate overlapping cells, which it might not able to count or have post-processing techniques due to the limitation of the technique.

C. Classification

RBC classifications firstly based on manual features, such as circularity, color average, diameter, area, etc. The features were used in rule-base methods [7], [8], [13], [16], K-nearest neighbor [21], and Artificial neural network (ANN) [9], [23], [29], [24], [10]. After that, convolutional neural network (CNN) [14], [30], [27], [31], [32], [33] have been used instead to auto generate features due to better computing power in nowadays, and it can extend to have more classes. Deformable U-net [26] were used to perform both segmentation and classification in a single model. In

the recent classification studies, the CNN classifiers have more layers and new techniques. Durant et al. [31] used DenseNet, which it has more than 150 layers, to predict 10 RBC types. [34] purposed multi-label detection using Faster-rcnn with Resnet to detect 6 types with touching and overlapping cells as a type. [6] used focal loss to classify 3 RBC types with imbalanced dataset.

According to the results in each study, the most updated trend is based on deep learning. The performance of the outcome mostly depends on the size and quality of the dataset that was used. Every study used their dataset to train and validate the result which is hard to compare. Moreover, the dataset still have small amounts of data because of the data collection mostly done in a hospital which is more difficult processes than general image dataset collection. For multi-class classification, some RBC types are rare to find so the dataset may have an imbalance problem. To classify the minority classes that have small data, imbalance techniques occurred to help the classification model not biased to the majority classes. Oversampling and undersampling are common techniques in the data level that was used to deal with the imbalance problem. [35] reviewed many imbalanced techniques on various data types on data level and algorithm level and shows that oversampling outperforms undersampling in most cases. Focal loss [3] is modified from the cross-entropy loss that helps the model training on hard miss-classified samples and less focuses on well-classified samples.

III. PROPOSED METHODS

In this section, the purpose method starts from normalizing the images, extracting an individual cell from blood smear images to identify the type of each RBCs, which is described by dividing into 4 main steps: 1. RBC color normalization, 2. Overlapping cell separation, 3. RBC contour extraction, and 4. RBC classification. The overall processes are shown in Figure 2.

A. Color normalization

In the data collection process, collectors might have different environments such as camera settings, microscope light levels, blood smear slide preparation, etc. The collectors also might collect multiple blood smear slides of a single RBC type at a time making each type has its own color space as shown in figure 2. Although, hematologists can disregard the difference in color space from expertise but the model can be biased from different color spaces during the training process instead of the characteristics of that type.

In this step, we extract backgrounds and find 3 overall average background values of RGB channels of all blood smear images, R_{avg} , G_{avg} , B_{avg} . Before training and predicting the results, the different values of 3 average background values of the target image k , r_{avg}^k , g_{avg}^k , b_{avg}^k , and the overall averages values were added to all pixels of the target image. The normalization equation of pixel (i, j) for image k are shown in equation 1. Although, the normalized images only were used for improving classification results. The huge improvement of the normalization in accuracy was shown in the results section.

$$\begin{aligned} r_{i,j}^k &= r_{i,j}^k + (R_{avg} - r_{avg}^k) \\ g_{i,j}^k &= g_{i,j}^k + (G_{avg} - g_{avg}^k) \\ b_{i,j}^k &= b_{i,j}^k + (B_{avg} - b_{avg}^k) \end{aligned} \quad (1)$$

B. RBC contour extraction

To extract RBC contours from blood smear images, first, the color RBC image is converted to a grayscale image using the green channel image from the RGB image, which grayscale has more contrast than other channels, as shown in Figure 3. CLAHE (Contrast Limited Adaptive Histogram Equalization), histogram equalization that applies to a small region which is divided uniformly, was used to enhance RBC regions out of the background. Then, Otsu threshold, and contour finding were used to extract cell regions. The overall process is shown in Figure 4.

C. Overlapping cells separation

In manual RBC analysis, hematologists typically avoid selecting the area in a blood smear slide that has overlapping cells to evaluate the result. It is simple to count and identify the type of RBCs when the border is not hidden behind other cells. To separate the overlapping RBCs, the most reliable methods based on distance transform and ellipse fitting. The distance transform is used to find the peak spots furthest from the border. The peak spots were used to identify a unique cell then several techniques, such as the random walk method and watershed transform, were used to find the area of each cell. However, the distance transform works effectively in a circular shape and a small group of overlapping cells, the peak area may coexist making it difficult to specify a certain amount. The ellipse fitting method uses the edge of RBC to approximate ellipse which identifies the area of RBC.

Our presented method is based on ellipse fitting. The overall process can divide into 4 steps:

1) *Concave point finding*: In each point of coordinate in the RBC contour, (x_i, y_i) , k middle points were calculated by finding the center of the distance between k pairs of contour points near the point. If all k points are outside the contour, the point is considered as a concave point. However, more than one concave points can be found in a wide curve, only one concave point was selected by averaging all near concave points. The concave points function, $f(x)$, were calculated as follows:

$$f(x_i, y_i) = \prod_{j=1}^k g\left(\frac{x_{i-j} + x_{i+j}}{2}, \frac{y_{i-j} + y_{i+j}}{2}\right) \quad (2)$$

$$g(x) = \begin{cases} 1, & (x, y) \text{ is outside a contour,} \\ 0, & (x, y) \text{ is inside a contour} \end{cases} \quad (3)$$

2) *Ellipse estimation*: For the contour has more than one concave point, curves between two concave points were used to approximate ellipse shape by direct ellipse fitting [36] based on the least-square method. The direct ellipse fitting is recommended instead of the original [37] which gives an approximate ellipse that does not relate to the curve in some conditions. The direct ellipse fitting has a constrain by ensuring that the discriminant, $4ac - b^2 = 0$ for the ellipse equation, as shown in equation 4.

$$ax^2 + bxy + cy^2 + dx + ey + f = 0 \quad (4)$$

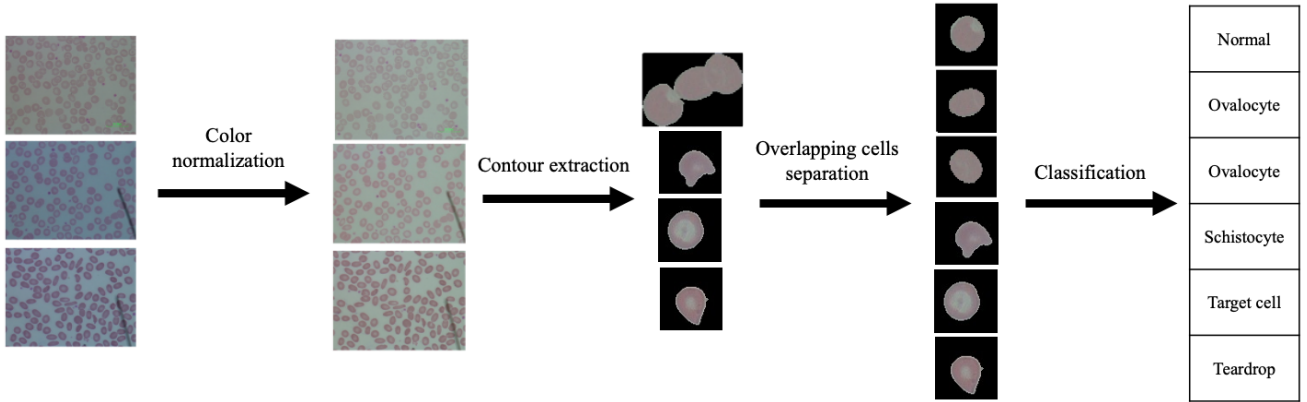


Fig. 2. Overall purposed method

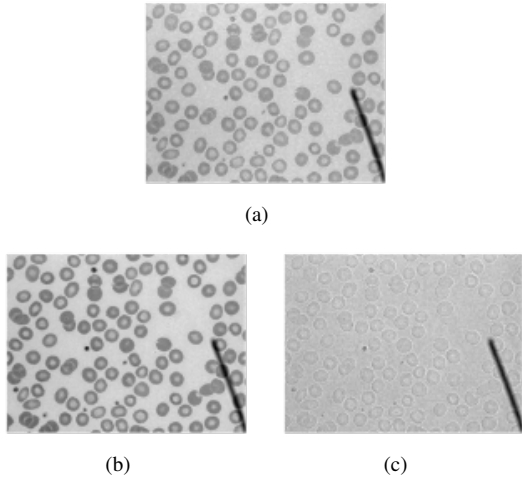


Fig. 3. (a) red channel image, (b) green channel image, (c) blue channel image

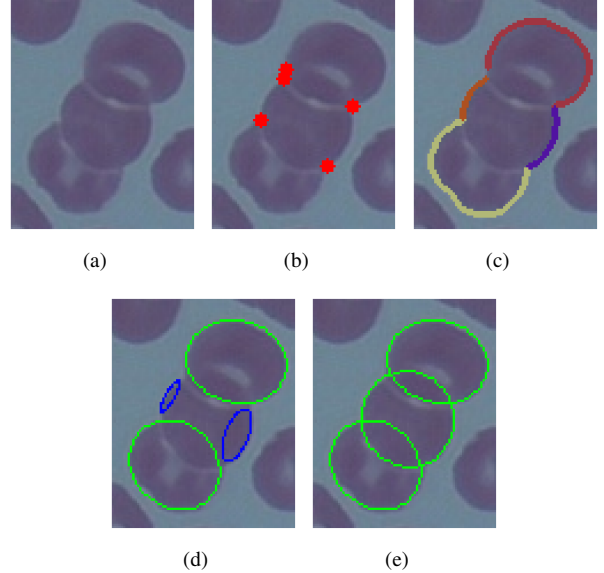


Fig. 5. Overlapping cells separation steps

of RBC. If there are more than two ellipses that not pass the conditions, then two curves were concatenated and used to estimate an ellipse of the remaining cell. 2 blue ellipses in figure 5(d) shows incorrect the cell estimation, and (e) shows the correct cell after ellipse fitting with 2 curves.

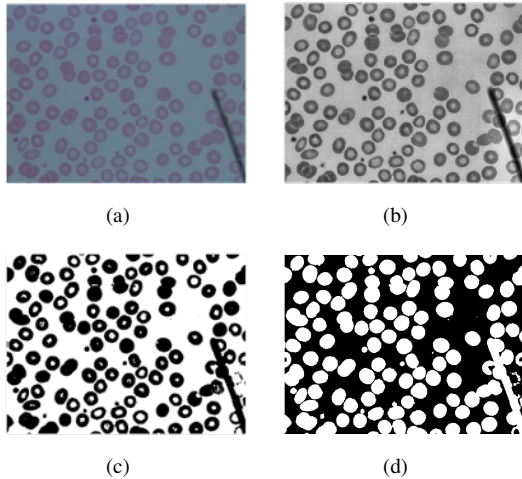


Fig. 4. (a) original image, (b) CLAHE image, (c) threshold image, (d) contour image

3) *Ellipse verification*: After finding all ellipse in each contour, the ellipses were sorted by area in descending order. Then, we verify each ellipse is in the RBC contour by two simple conditions: 80% of the ellipse area is in the contour and 20% of the ellipse area is in the remaining area in the contour does not in previous ellipses.

4) *Two curve ellipse estimation*: In highly overlapping RBCs, the cells overlap each other more than two cells, curves might not able to restore the correct ellipse shape

D. RBC classification

In this step, single contour images were created to feed the deep learning model. In our dataset, it has 12 classes of RBCs: 11 RBC types and an uncategorized class which is the other types of RBC. The dataset was labeled by specialists in hematology. The numbers of RBCs in each class are shown in Table I. Figure 1 shows RBC images in each type. The dataset is highly imbalanced because some classes are found in rare such as Teardrop, Sickle cell, and Uncategorized.

1) *EfficientNet*: For classification, we used pretrained EfficientNet model [2] which showed remarkable accuracy and better performance than the older models. It was designed by carefully balancing network depth, width, and resolution. the model has 8 different sizes: EfficientNet-b0 to EfficientNet-b7. In the result section, the EfficientNet-b0 to EfficientNet-b4 were observed with 5 fold-cross validation with 80% and 20% for training and testing. Moreover, we used data augmentation and weight initial-

TABLE I
TOTAL NUMBER OF CLASS IN RBC DATASET

RBCs Class	Total number of RBCs
Normal	6286
Macrocyte	687
Microcyte	459
Spherocyte	3445
Target cell	2703
Stomatocyte	1991
Ovalocyte	2137
Teardrop	305
Burr cell	783
Schistocyte	861
Hypochromia	1036
Uncategorised	182
Total	20875

ization to observe which technique could overcome the class imbalance problem. Only random flips and rotates were used for data augmentation because the RBC classes are sensitive for size and color such as Normal Macrocyte and Microcyte are different in size.

To evaluate performance, accuracy is commonly used for image classification. For the imbalanced dataset, the accuracy is insufficient, it can be dominated by the majority classes. However, many metrics [35] were used to describe the imbalanced dataset. F1-score was used in this experiment. It is a well-known metric that balances precision and recall by harmonic mean that sensitizes to the minority classes.

2) *Imbalanced techniques*: Further analysis on imbalanced dataset was done. It is a common problem for biomedical dataset. Our dataset also have highly imbalance with 34.538 imbalance ratio on 12 classes with 20,875 (calculated from highest sample class/lowest sample class). In training step the model can be overcome by high sample classes but less focus on low sample classes. The weight balancing, up sampling, and focal loss are investigated in this study.

For weight balancing, normally, every classes have the same weight, 1.0. The weight balancing helps a model balance learning gradients in backpropagation step between high sample classes and low sample class, high weight on low sample classes and low weight on high sample classes. In our experiments, each class has weight $\frac{1}{f}$, $\frac{1}{\sqrt{f}}$, and $\frac{1}{\sqrt[3]{f}}$ as weight1, weight2, and weight3 while f is amount of sample in the class.

For up sampling, it makes every class has the same amount of sample by replicating its own data. It would help the trained model not overcome by high sample classes. In this case, every class were replicate itself to match the normal class.

Focal loss is used to help the model focus on high loss and reduce the loss near 0. It was used in object detection task which highly imbalance between objects and non-object classes. We were used to investigate on this problem, which is multi-class classification, whether it helps in imbalanced multi-classification. As shown in equation 5 focal loss has added term from cross entropy loss which reduce loss when the predicted probability result close to grown truth by γ hyperparameter.

$$FL(p_t) = -(1 - p_t)^\gamma \log(p_t) \quad (5)$$

TABLE II
OVERLAPPING CELLS SEPARATION RESULT

Contour	Correct	Incorrect (Concave)	Incorrect (Fitting)	Total
2 RBCs	185	18	4	207
3 RBCs	38	2	1	41
>3 RBCs	23	2	4	29
Total	246	22	9	277

TABLE III
RBC CLASSIFICATION RESULTS

Model	Accuracy	F1-score
efficientnet-b0	0.8821	0.8378
efficientnet-b1	0.8823	0.8426
efficientnet-b2	0.8842	0.8399
efficientnet-b3	0.8819	0.8423
efficientnet-b4	0.8830	0.8405
efficientnet-b0-aug	0.8996	0.8639
efficientnet-b1-aug	0.9021	0.8679
efficientnet-b2-aug	0.8988	0.8636
efficientnet-b3-aug	0.9001	0.8642
efficientnet-b4-aug	0.8990	0.8668

IV. IMPLEMENTATIONS

The blood smear image size in our dataset is 640 * 480 pixels. For the overlapping cells separation step, the k value is 8. RBC contours were crop and put on a blank 72 * 72 image which is big enough to contain the biggest cell.

For classification, the contour images were scaled to 224 * 224 which is the input size of EfficientNet model. The models were trained with pretrained parameters. The learning rate was 0.001 with 0.1 learning decay rate in every 15 epochs. The total epochs are 100.

V. RESULTS

In this section, Overlapping cells separation and RBC classification results were provided and analyzed.

A. Overlapping cells separation

To evaluate the separation of the overlapping cells, we manually counted the overlapping contours which do not contain the cell on the border of the images and other artifacts such as platelets, white blood cells, or microscope tools in images. 277 contours were found in 20 blood smear images. The overall accuracy is 0.889. Most of the contours are 2 RBCs touch or overlap each other. The error in our method was mostly found on the contour that was found only 1 concave point. The results are shown in Table II. Blood smear images after segmentation are shown in figure 6.

B. RBC Classification

In the first step, we investigated on model sizes, EfficientNet-b0 to b4 using augmentation and without augmentation. The results on table III show that EfficientNet-b1 with augmentation has highest accuracy and f1-score. As the result, increase the model size is not significant improving the performance. The limitation is the sample size of dataset. Increase the model size can lead into overfit problem. Therefore, imbalance techniques were investigated, including weight balancing, up sampling, and Focal loss with EfficientNet-b1 as a baseline.

Training overall accuracy and f1-score of EfficientNet-b1 with imbalance techniques are shown in table IV.

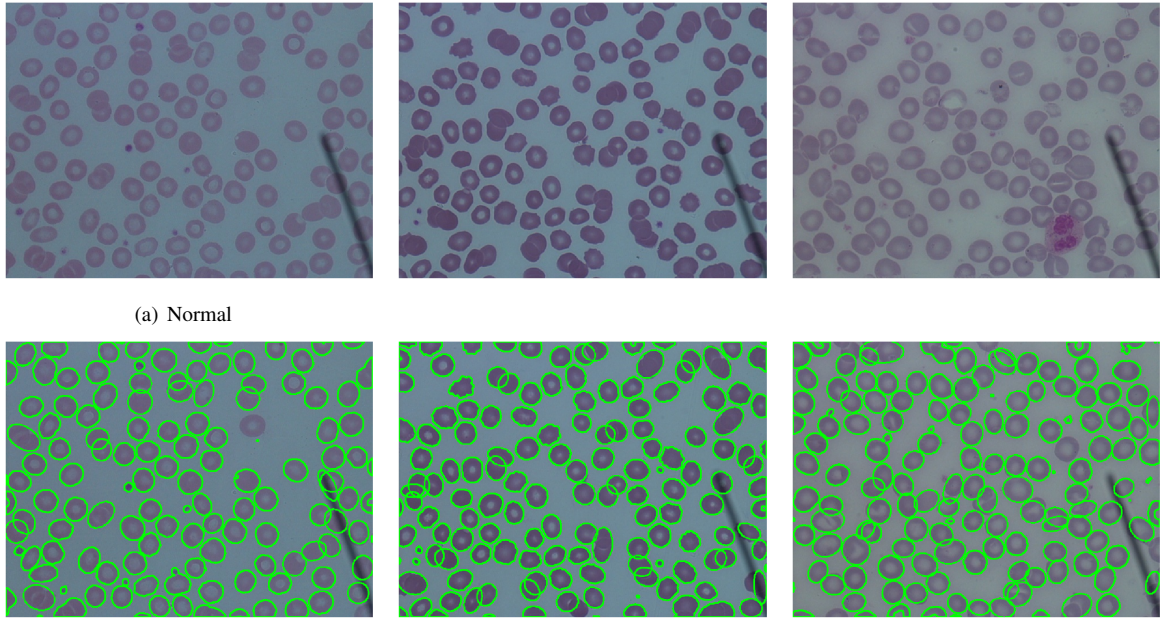


Fig. 6. Segmentation results

TABLE IV

EFFICIENTNET-B1 WITH IMBALANCE TECHNIQUES ACCURACY AND F1-SCORE

Model	Accuracy	F1-score
Baseline	0.8823	0.8426
Aug	0.9021	0.8679
Weight	0.8752	0.8374
Weight2	0.8808	0.8435
Weight3	0.8820	0.8410
AugWeight	0.8698	0.8344
AugWeight2	0.8954	0.8630
AugWeight3	0.8981	0.8672
Up	0.8772	0.8403
AugUp	0.8877	0.8591
AugFocal0.5	0.8947	0.8523
AugFocal1.0	0.8932	0.8510
AugFocal1.5	0.8926	0.8543
AugFocal2.0	0.8900	0.8480
AugFocal2.5	0.8884	0.8486
AugFocal3.0	0.8877	0.8488

However, the baseline model with augmentation still has highest accuracy and f1-score with AugWeight3 (augmentation and $\frac{1}{\sqrt[3]{f}}$ weight) is the second. Up (Up sampling) shows slightly lower result from a baseline while AugUp (Aumentation with up sampling) shows slightly better. Augmentation with focal loss results with different γ hyperparameter (AugFocal0.5 - AugFocal3.0) was shown that the result decrease when increase the hyperparameter.

Tabel V shows the f1 score in each class. The results had shown that Aug improves all class f1 score from the baseline. Weight - Weight3 and AugWeight - AugWeight3 shows similar result compared with the baseline and Aug respectively. AugWeight3 has 6 classes better f1 score than Aug. It can imply that extremely different weight might not show a good result. AugUp has 3 classes better than Aug with huge improvement in Teardrop and Uncategorized. Focal loss shows decreasing result when increasing the γ hyperparameter in all classes.

In summary, the difference between this dataset and general dataset in classification problem are the dataset that imbalanced and RBC classes that has many similar

characteristics. Almost all classes has circular shape, only few characteristic that different such as size, shape, color. The best result is the EfficientNet-b1 with augmentation. Further analysis on imbalance dataset, Weight balancing and focal loss are done in loss function. Weight balancing helps improve the low samples classes and less focus on high sample classes. Otherwise, focal loss show decrease performance for this dataset because it focuses on high value loss but the RBC classes are almost similar shape so the loss is almost entirely in the middle which is ignored. Up sampling is done in data level, similar to augmentation. This technique seem to work best in unique shape classes which is teardrop cell and uncategorized.

In table VI shows analysis in normalization step whether it helps to improve the performance. The result show huge improvement from augmentation with unnormalize image. We also train the model with different background colors which is black, white, gray, and the average background color. The black background shows the best result while others shows slightly lower.

VI. CONCLUSION & FUTURE WORKS

we present a simple method to segment RBCs that have ability to separate overlapping cells based on concave points, and classify RBCs into 12 classes. The process start from color normalization which reduce the color space and making the trained model do not biased on color. Contour extraction is a step to extract RBC contour are out of background. The next step is overlapping cells separation using new method to find concave points and using the direct ellipse fitting to estimate the single shape of RBC. Lastly, classification using EfficientNet-b1 show best result with augmentation. Moreover, further analysis for handing imbalanced dataset has shown that weight balancing has ability to reduce bias of trained model on the majority classes.

Many deep learning studies on RBC still lack of standard public dataset to evaluate the performance. Our dataset

TABLE V
EFFICIENTNET-B1 WITH IMBALANCE TECHNIQUES RESULT IN CLASSES

Techniques	Normal	Macro	Micro	Spher	Target	Stoma	Ovalo	Tear	Burr	Schis	Uncat	Hypo
Baseline	88.11	81.76	65.43	93.11	93.47	89.96	88.99	81.88	85.67	81.26	84.66	76.84
Aug	90.23	84.87	68.50	94.56	94.08	91.68	91.28	88.40	87.83	85.28	84.99	79.80
Weight	87.19	81.31	66.75	92.79	92.56	88.79	88.66	80.60	86.58	80.90	83.23	75.49
Weight2	87.63	83.08	64.17	93.31	93.19	89.67	89.42	82.00	86.54	80.52	86.04	76.64
Weight3	88.04	82.05	64.39	93.12	93.33	90.51	89.47	82.58	84.95	81.78	83.33	75.68
AugWeight	85.00	79.19	62.10	92.95	93.48	90.20	90.25	86.85	86.14	83.64	75.27	76.26
AugWeight2	89.00	82.67	68.88	94.23	94.22	91.69	90.89	87.38	87.53	84.41	84.85	79.91
AugWeight3	89.43	82.82	67.98	94.07	94.26	91.83	91.18	89.36	88.14	85.52	86.26	79.74
Up	87.87	79.46	60.36	92.86	93.36	88.67	89.10	86.44	82.28	80.98	90.14	76.81
AugUp	88.74	79.34	65.19	93.85	94.17	88.73	90.47	92.44	84.18	82.94	92.96	77.94
AugFocal0.5	89.28	83.37	63.89	93.94	94.30	91.62	91.12	85.91	87.36	82.93	80.47	78.52
AugFocal1.0	89.25	82.37	65.29	94.09	93.99	91.01	90.67	83.46	87.38	83.83	82.05	77.77
AugFocal1.5	88.89	83.10	66.48	93.68	94.24	91.01	91.14	85.32	87.34	83.43	82.64	77.88
AugFocal2.0	88.73	82.50	66.89	93.95	93.72	91.12	90.86	85.38	86.74	82.01	79.00	76.69
AugFocal2.5	88.37	82.72	67.53	93.66	94.01	90.15	91.18	84.90	85.83	83.12	80.38	76.49
AugFocal3.0	88.34	81.99	66.35	93.71	93.55	90.14	90.48	83.76	87.41	82.15	82.38	78.25

TABLE VI
EFFICIENTNET-B1 WITH DIFFERENCE NORMALIZE TECHNIQUES

Model	Accuracy	F1-score
AugUnnormalize	0.6325	0.4241
AugBlackbg	0.9021	0.8679
AugWhitebg	0.8977	0.8634
AugGraybg	0.8969	0.8603
AugAVGbg	0.8979	0.8626

have more sample and more types than many studies but still need to improve the imbalanced problems. We have planned to public the dataset in near future. For our method, we used the lasted model EfficientNet to classify the RBCs, however segmentation step still is not learning based method which is a trend and shown better result in many specific computer vision area. Future work would uses object detection method to find bounding box and classify the RBCs.

ACKNOWLEDGMENT

This research is funded by "Newton Fund" and Ratchadaphiseksomphot Endowment Fund Chulalongkorn University.

REFERENCES

- [1] J. Ford. Red blood cell morphology. *International Journal of Laboratory Hematology*, 35(3):351–357, 2013.
- [2] Mingxing Tan and Quoc V. Le. EfficientNet: Rethinking model scaling for convolutional neural networks.
- [3] Tsung-Yi Lin, Priya Goyal, Ross Girshick, Kaiming He, and Piotr Dollár. Focal loss for dense object detection.
- [4] Roopa B. Hegde, Keerthana Prasad, Harishchandra Hebbar, and I Sandhya. Peripheral blood smear analysis using image processing approach for diagnostic purposes: A review. *Biocybernetics and Biomedical Engineering*, 38(3):467–480, January 2018.
- [5] S. M. Mazalan, N. H. Mahmood, and M. A. A. Razak. Automated Red Blood Cells Counting in Peripheral Blood Smear Image Using Circular Hough Transform. In *Modelling and Simulation 2013 1st International Conference on Artificial Intelligence*, pages 320–324, December 2013.
- [6] Kitsuchart Pasupa, Supawit Vatathanavaro, and Suchat Tungjintob. Convolutional neural networks based focal loss for class imbalance problem: a case study of canine red blood cells morphology classification.
- [7] Ramin Soltanzadeh and Hossein Rabbani. Classification of three types of red blood cells in peripheral blood smear based on morphology. In *IEEE 10th INTERNATIONAL CONFERENCE ON SIGNAL PROCESSING PROCEEDINGS*, pages 707–710. ISSN: 2164-523X.
- [8] S. Chandrasiri and P. Samarasinghe. Automatic anemia identification through morphological image processing. In *7th International Conference on Information and Automation for Sustainability*, pages 1–5, December 2014.
- [9] Razali Tomari, Wan Nurshazwani Wan Zakaria, Muhammad Madih Abdul Jamil, Faridah Mohd Nor, and Nik Farhan Nik Fuad. Computer Aided System for Red Blood Cell Classification in Blood Smear Image. *Procedia Computer Science*, 42:206–213, January 2014.
- [10] Howard Lee and Yi-Ping Phoebe Chen. Cell morphology based classification for red cells in blood smear images. *Pattern Recognition Letters*, 49:155–161, November 2014.
- [11] Miguel Romero-Rondán, Laura Sanabria-Rosas, Lola Bautista-Rozo, and Alfonso Mendoza. Algorithm for detection of overlapped red blood cells in microscopic images of blood smears. 83:188–195.
- [12] I. Ahmad, S. N. H. S. Abdullah, and R. Z. Azma Raja Sabudin. Geometrical vs spatial features analysis of overlap red blood cell algorithm. In *2016 International Conference on Advances in Electrical, Electronic and Systems Engineering (ICAES)*, pages 246–251, November 2016.
- [13] Vasundhara Acharya and Preetham Kumar. Identification and red blood cell classification using computer aided system to diagnose blood disorders. In *2017 International Conference on Advances in Computing, Communications and Informatics (ICACCI)*, pages 2098–2104.
- [14] Gopalakrishna Pillai Gopakumar, Murali Swetha, Gorthi Sai Siva, and Gorthi R. K. Sai Subrahmanyam. Convolutional neural network-based malaria diagnosis from focus stack of blood smear images acquired using custom-built slide scanner. *Journal of Biophotonics*, 11(3):e201700003, 2018.
- [15] Mamata Anil Parab and Ninad Dileep Mehendale. Red blood cell classification using image processing and CNN. page 2020.05.16.087239. Publisher: Cold Spring Harbor Laboratory Section: New Results.
- [16] Virginia Mari E. Batitis, Merwin Jhan G. Caballes, Abigail A. Ciudad, Miccuela D. Diaz, Russel D. Flores, and Engr. Roselito E. Tolentino. Image classification of abnormal red blood cells using decision tree algorithm. In *2020 Fourth International Conference on Computing Methodologies and Communication (ICCMC)*, pages 498–504.
- [17] Pranati Rakshit and Kriti Bhowmik. Detection of Abnormal Findings in Human RBC in Diagnosing Sickle Cell Anaemia Using Image Processing. *Procedia Technology*, 10:28–36, January 2013.
- [18] Nicola Ritter and James Cooper. Segmentation and Border Identification of Cells in Images of Peripheral Blood Smear Slides. In *Proceedings of the Thirtieth Australasian Conference on Computer Science - Volume 62, ACSC '07*, pages 161–169, Darlinghurst, Australia, Australia, 2007. Australian Computer Society, Inc. event-place: Ballarat, Victoria, Australia.
- [19] S. Kareem, R. C. S. Morling, and I. Kale. A novel method to count the red blood cells in thin blood films. In *2011 IEEE International Symposium of Circuits and Systems (ISCAS)*, pages 1021–1024, May 2011.
- [20] Mehdi Habibzadeh, A. Krzyzak, Thomas Fevens, and Ali Sadr. Counting of RBCs and WBCs in noisy normal blood smear microscopic images. volume 7963, March 2011.
- [21] V. Sharma, A. Rathore, and G. Vyas. Detection of sickle cell anaemia and thalassaemia causing abnormalities in thin smear of human blood sample using image processing. In *2016 International Conference on Inventive Computation Technologies (ICICT)*, volume 3, pages 1–5, August 2016.
- [22] R. Cai, Q. Wu, R. Zhang, L. Fan, and C. Ruan. Red blood cell

- segmentation using Active Appearance Model. In *2012 IEEE 11th International Conference on Signal Processing*, volume 3, pages 1641–1644, October 2012.
- [23] Hanung Adi Nugroho, Son Ali Akbar, and E. Elsa Herdiana Murhandarwati. Feature extraction and classification for detection malaria parasites in thin blood smear. In *2015 2nd International Conference on Information Technology, Computer, and Electrical Engineering (ICITACEE)*, pages 197–201.
- [24] Dyah Aruming Tyas, Tri Ratnarningsih, Agus Harjoko, and Sri Hartati. The Classification of Abnormal Red Blood Cell on The Minor Thalassemia Case Using Artificial Neural Network and Convolutional Neural Network. In *Proceedings of the International Conference on Video and Image Processing, ICVIP 2017*, pages 228–233, New York, NY, USA, 2017. ACM. event-place: Singapore, Singapore.
- [25] A. Sadafi, M. Radolko, I. Serafeimidis, and S. Hadlak. Red Blood Cells Segmentation: A Fully Convolutional Network Approach. In *2018 IEEE Intl Conf on Parallel Distributed Processing with Applications, Ubiquitous Computing Communications, Big Data Cloud Computing, Social Computing Networking, Sustainable Computing Communications (ISPA/IUCC/BDCloud/SocialCom/SustainCom)*, pages 911–914, December 2018.
- [26] Mo Zhang, Xiang Li, Mengjia Xu, and Quanzheng Li. Image Segmentation and Classification for Sickle Cell Disease using Deformable U-Net. *arXiv:1710.08149 [cs, q-bio]*, October 2017. arXiv: 1710.08149.
- [27] Mengjia Xu, Dimitrios P. Papageorgiou, Sabia Z. Abidi, Ming Dao, Hong Zhao, and George Em Karniadakis. A deep convolutional neural network for classification of red blood cells in sickle cell anemia. *PLOS Computational Biology*, 13(10):e1005746, 2017.
- [28] M. González-Hidalgo, F. A. Guerrero-Peña, S. Herold-García, A. Jaume-i Capó, and P. D. Marrero-Fernández. Red Blood Cell Cluster Separation From Digital Images for Use in Sickle Cell Disease. *IEEE Journal of Biomedical and Health Informatics*, 19(4):1514–1525, July 2015.
- [29] Adnan Khashman. IBCIS: Intelligent blood cell identification system. *Progress in Natural Science*, 18(10):1309–1314, October 2008.
- [30] Z. Liang, A. Powell, I. Ersoy, M. Poostchi, K. Silamut, K. Palaniappan, P. Guo, M. A. Hossain, A. Sameer, R. J. Maude, J. X. Huang, S. Jaeger, and G. Thoma. CNN-based image analysis for malaria diagnosis. In *2016 IEEE International Conference on Bioinformatics and Biomedicine (BIBM)*, pages 493–496, December 2016.
- [31] Thomas J. S. Durant, Eben M. Olson, Wade L. Schulz, and Richard Torres. Very Deep Convolutional Neural Networks for Morphologic Classification of Erythrocytes. *Clinical Chemistry*, 63(12):1847–1855, December 2017.
- [32] M. Z. Alom, C. Yakopcic, T. M. Taha, and V. K. Asari. Microscopic Blood Cell Classification Using Inception Recurrent Residual Convolutional Neural Networks. In *NAECON 2018 - IEEE National Aerospace and Electronics Conference*, pages 222–227, July 2018.
- [33] Prayag Tiwari, Jia Qian, Qiuchi Li, Benyou Wang, Deepak Gupta, Ashish Khanna, Joel J. P. C. Rodrigues, and Victor Hugo C. de Albuquerque. Detection of subtype blood cells using deep learning. *Cognitive Systems Research*, 52:1036–1044, December 2018.
- [34] Wei Qiu, Jiaming Guo, Xiang Li, Mengjia Xu, Mo Zhang, Ning Guo, and Quanzheng Li. Multi-label detection and classification of red blood cells in microscopic images.
- [35] Justin M. Johnson and Taghi M. Khoshgoftaar. Survey on deep learning with class imbalance. 6(1):27.
- [36] A. Fitzgibbon, M. Pilu, and R.B. Fisher. Direct least square fitting of ellipses. 21(5):476–480. Conference Name: IEEE Transactions on Pattern Analysis and Machine Intelligence.
- [37] Aw Fitzgibbon and Rb Fisher. A buyer's guide to conic fitting. In *Proceedings of the British Machine Vision Conference 1995*, pages 51.1–51.10. British Machine Vision Association.